Optical phonons polarized along the c axis of $YBa_2Cu_3O_{6+x}$, for x = 0.5 → 0.95[*]

C.C. Homes[†] and T. Timusk[‡]

Department of Physics and Astronomy, McMaster University, Hamilton, Ontario, Canada L8S 4M1

D.A. Bonn, R. Liang and W.N. Hardy

Department of Physics, University of British Columbia, Vancouver, B.C., Canada V6T 2A6

(April 24, 1995)

The c-axis polarized phonon spectra of single crystals of $YBa_2Cu_3O_{6+x}$, have been measured for the doping range $x = 0.5 \rightarrow 0.95$, between 10 K and 300 K. The low background electronic conductivity, determined by Kramers-Kronig analysis of the reflectance, leads to a rich phonon structure. With decreased doping the five normally-active B_{1u} modes broaden and the high-frequency apical oxygen mode splits into two components. We associate the higher of these with the two-fold coordinated copper "sticks". The 155 cm^{-1} low-frequency mode, which involves the apical and the chain-oxygens, splits into at least three components with decreasing doping. Some phonon anomalies which occur near T_c in the highly-doped material occur well above T_c in the oxygen-reduced systems. An unusual broad phonon band develops in the normal state at ≈ 400 cm^{-1}, which becomes more intense at low doping and low temperatures, borrowing oscillator strength from apical and plane oxygen modes resulting in a major transformation of the phonon spectrum below ≈ 150 K.

PACS numbers: 78.30.Er,74.70.Vy,74.30.Gn

I. INTRODUCTION

The role of phonons in high-temperature superconductors is complex. On the one hand there is ample evidence that the cuprates are not conventional electron-phonon BCS superconductors. This evidence includes, for the optimally doped materials a linear resistivity, in the normal state, with a zero-temperature intercept at zero resistance,[1,2] a collapse of transport scattering at the superconducting transition,[3–5] and a lack of an isotope effect.[6–9]

On the other hand, a large number of studies show that certain phonons at least are coupled to the carriers, and that this coupling is unconventional.[10,11] The frequencies and widths of certain phonon lines, again in the optimally-doped materials (precisely those where the isotope effect is small), undergo abrupt changes at T_c. This effect was first observed by infrared spectroscopy,[12–15] then by Raman spectroscopy[15–17], resonant neutron-absorption spectroscopy[18] and neutron scattering.[19]

Broad minima in the ab-plane optical conductivity are seen at frequencies that are in the phonon region. These have been shown to be associated with c-axis longitudinal optic (LO) phonons[20,21] that couple to the ab-plane conductivity by a symmetry-breaking mechanism.

In this paper we focus on the changes in the c-axis phonon spectra of $YBa_2Cu_3O_{6+x}$ as we change the oxygen doping. These spectra can be separated from the weak and smooth electronic background conductivity whose intensity rises with doping from a few Ω^{-1}cm^{-1} in the $x = 0.5$ material[22] to 450 Ω^{-1}cm^{-1} in over-doped samples.[23] The background is due to inter-cell hopping of free carriers.[24] Superimposed on this electronic background are five strong phonon lines. These five lines are also seen the in the spectra of ceramic superconductors,[25,26] and have been studied by a large number of groups. The extensive literature on ceramic spectra has been summarized by Feile.[27] However, in ceramics, effects due to the background ab-plane conductivity distort the spectra, particularly the line strengths, and the c-axis polarized phonons are best studied in single crystals. Single crystal studies are difficult due to the small area of the available flux-grown samples. Nevertheless, a number of studies have appeared, with $YBa_2Cu_3O_{6+x}$ being the most studied material.[22,23,28–33] In the present work single crystals with cleaved surfaces are used and the region of doping ranges from the optimally doped, that is the material with the highest $T_c = 93.5$ K with $x = 0.95$, to an underdoped sample with $x = 0.5$ which is still superconducting with a $T_c = 53$ K. Preliminary reports of this work have been published,[33–35] and the electronic background is the subject of a separate publication.[22]

II. EXPERIMENTAL DETAILS

A. Experimental

The spectra were obtained by a Kramers-Kronig transformation of c-axis polarized reflectance of millimeter-size, high-quality single crystals. The growth of the single crystals and experimental techniques used have been reported on previously.[33,36] To maximize the signal from
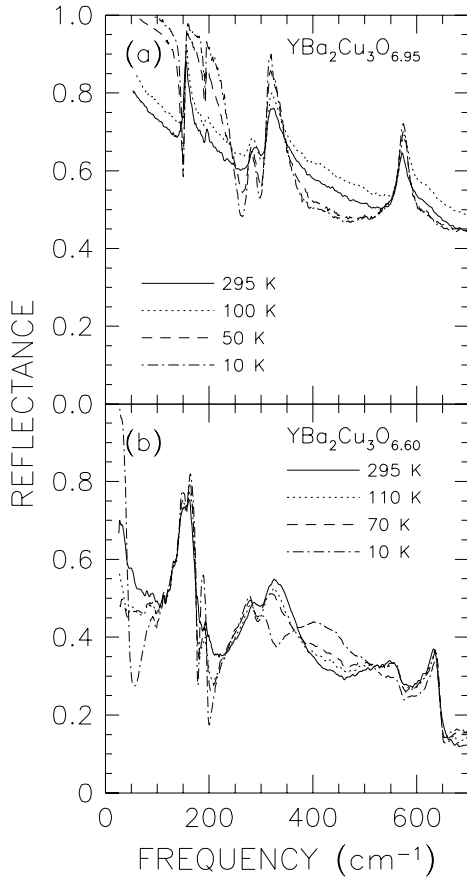
FIG. 1. The reflectance of $YBa_2Cu_3O_{6+x}$ for radiation polarized along the c axis from ≈ 50 cm^{-1} to 700 cm^{-1} at several temperatures above and below T_c, for two oxygen dopings x: (a) fully-doped material with $x = 0.95$ ($T_c = 93$ K), and (b) an underdoped crystal with $x = 0.6$ ($T_c = 58$ K). The main change in the phonon spectrum in the underdoped material is a new line at 610 cm^{-1} that we associate with the bridging oxygen at the two-fold coordinated copper sites in the chain layer. Another new feature in the $x = 0.6$ material is a broad band at ≈ 400 cm^{-1} that appears at low temperature.

FIG. 2. The optical conductivity (σ_1) at 295 K for $YBa_2Cu_3O_{6+x}$ for radiation polarized along the c axis from ≈ 50 cm^{-1} to 700 cm^{-1} for five oxygen dopings, $x = 0.5 \rightarrow 0.95$. As the doping is reduced, the background conductivity is reduced uniformly at all frequencies. At high frequency, in addition to the apical oxygen [O(4)] peak at 570 cm^{-1} a new phonon peak grows at ≈ 610 cm^{-1}; this peak is associated with the O(4) mode and the growing density of two-fold coordinated copper sites in the underdoped materials. As the doping is reduced, the O(4) modes acquire an increasingly dispersive line shape.

the ac face of the crystal, an infrared beam larger than signal from the ac face of the crystal, an infrared beam larger than the crystal was used. The sample was coated with gold *in situ* and then remeasured at each temperature to obtain a reference spectrum.[37]

The reflectance of $YBa_2Cu_3O_{6+x}$, for two oxygen concentrations, $x = 0.6$ and 0.95, for light polarized parallel to the c axis is shown in the phonon frequency range in Fig. 1 at several temperatures. The reflectance has a continuous background, rising towards unity at low frequency, characteristic of a poor metal, with sharp resonances due to optical phonons. In the superconducting state, the development of the superconducting condensate has the effect of producing a reflectance edge which shifts down to lower frequency as the doping is reduced. Also, as the temperature is lowered, the shapes of the
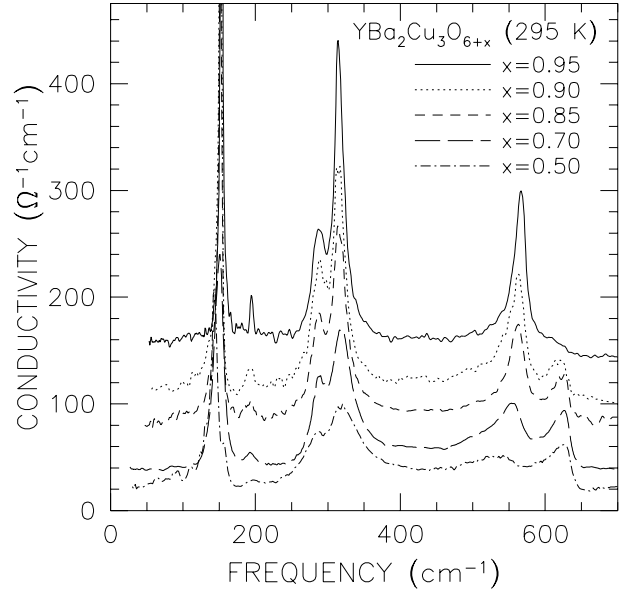
phonon features change due to the changing background conductivity.

Changes in oxygen doping have two principal effects on the phonon spectra: first, as the doping level is lowered, a new phonon feature appears at ≈ 610 cm^{-1}. Secondly, a very broad feature, weak at first, but stronger at low oxygen dopings, appears in the normal state at ≈ 400 cm^{-1}, and becomes stronger at low temperature. These effects are seen more clearly in the optical conductivity, discussed in the following section.

B. Optical conductivity

A Kramers-Kronig transformation of the reflectance was used to calculate the optical conductivity. The reflectance was extended to regions outside the actual measurements as follows: below the lowest measured frequency Hagen-Rubens frequency dependence: $[(1 - R) \propto \omega^{-1/2}]$ was assumed to hold in the normal state. In the superconducting state, where a plasma edge develops, it was assumed that the reflectance was given by
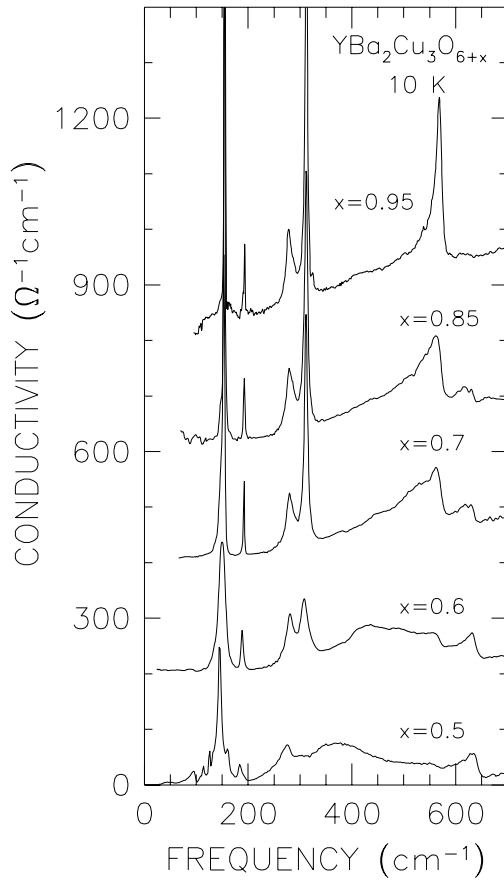
FIG. 3. The c-axis optical conductivity (σ_1) at 10 K for five oxygen dopings, $x = 0.5 \rightarrow 0.95$. The curves have been offset vertically in 200 Ω^{-1}cm^{-1} increments for clarity. There is a major redistribution of spectral weight from the O(4) peaks at ≈ 570 cm^{-1} and ≈ 610 cm^{-1}, and the in-plane buckling mode at 310 cm^{-1}, to an new broad band in the ≈ 400 cm^{-1} range. The peak shifts to lower frequency as the doping is reduced, starting as a shoulder on the apical-oxygen line at 550 cm^{-1} and ending up centered at ≈ 375 cm^{-1} in the $x = 0.5$ sample.

$(1 - R) \propto \omega^{-2}$. This assumes that the conductivity is finite and constant to zero frequency. There is good evidence from comparisons with transport measurements that both assumptions are valid.[22] Temperature dependent reflectance measurements were carried out to 5000 cm^{-1}. The room temperature measurements of Koch *et al.*[30] were used from 5000 cm^{-1} to 3.5×10^5 cm^{-1} and above this frequency free-electron behavior was assumed: $R \propto \omega^{-4}$.

The 295 K conductivity along the c-axis is shown in Fig. 2 for a wide range of dopings. The 10 K conductivity is shown in Fig. 3. Superimposed on a continuous background that increases in strength with doping are a series of sharp phonon lines. In general, the strength of the phonon bands does not depend strongly on doping, but as the doping is reduced a new phonon appears at ≈ 610 cm^{-1} in the nearly fully-doped material and

moves to higher frequency as the oxygen concentration is reduced. We will call this the 610 cm^{-1} line in what follows, but its actual frequency changes with doping and is as high as 635 cm^{-1} in the $x = 0.5$ material. The other major effect of doping occurs at low temperature where a new broad band appears at 400 cm^{-1} as the doping level is reduced to $x = 0.7$. This band seems to increase its oscillator strength at the expense of the two high-frequency modes and the band at 310 cm^{-1}. Also, its center frequency appears to decrease as the doping is reduced, reaching a value of ≈ 375 cm^{-1} in the $x = 0.5$ crystal.

III. RESULTS

A. Calculation of the phonon parameters.

In what follows we refer to the six phonons that we observe by their room temperature frequencies in the fully-doped material, bearing in mind that the actual center frequencies change with both temperature and doping. There are five strong phonons, and at room temperature their frequencies are: 155, 194, 279, 312 and 570 cm^{-1}, plus a weaker one at 610 cm^{-1}. All the lines have symmetric line shapes except for the two highest ones. The 570 cm^{-1} and the 610 cm^{-1} lines have Lorentzian shapes at room temperature, but at low temperature they become asymmetric.[38] Such lines are usually described in terms of a Fano line shape $\sigma_1(\omega) = A[(x + q)^2/(1 + x^2)]$, where $\sigma_1(\omega)$ is the conductivity, A is a constant, $x = (\omega - \omega_i)/\gamma_i$, ω_i is the phonon frequency, γ_i is the phonon line width and q_i is a parameter that describes the asymmetry of the ith phonon.[39]

While the Fano line shape describes the 570 cm^{-1} phonon at low temperatures, it fails as the line shape becomes more Lorentzian ($q \rightarrow \infty$). A better fit to the data is in terms of a classical Drude-Lorentz model for the dielectric function, for each phonon band, but with an empirical line shape made up of a mixture of the real and imaginary parts of the Lorentzian oscillator:

$$\tilde{\epsilon}(\omega) = \frac{\omega_p^2 e^{i\theta}}{\omega_{TO}^2 - \omega^2 + i\omega\gamma}, \tag{1}$$

where ω_p is the effective plasma frequency, ω_{TO} the center frequency and γ the width of the phonon. The parameter θ is the phase associated with the asymmetry of the phonon. The line shape is that of a classical oscillator for $\theta = 0$ but becomes asymmetric for nonzero θ.

An advantage of this rotated-Lorentzian line shape over the Fano profile is that one can associate with it an oscillator strength. For a pure Lorentzian the integrated oscillator strength is defined to be $\omega_p^2/8$; for the rotated Lorentzian, to leading order the oscillator strength is $\cos(\theta)\omega_p^2/8$, so that for small rotations, the introduction of an asymmetric line shape does not alter the oscillator sum rule too much. However, for rotations of greater
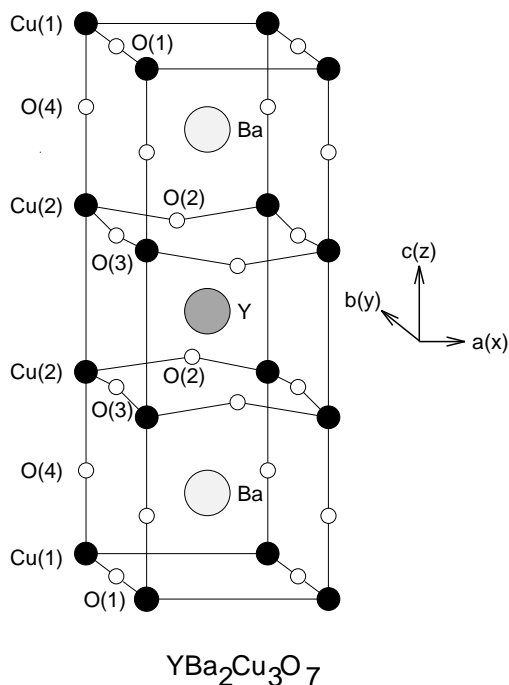
FIG. 4. The orthorhombic unit cell of $YBa_2Cu_3O_7$. The chain oxygen is denoted as O(1), the apical copper as Cu(1), and the O(4) as the apical oxygen atom. When all the O(1) sites are occupied, the Cu(1) atom is four-fold coordinated. Deoxygenation results in the oxygens at the O(1) sites being removed, lowering the coordination of the Cu(1) atom.

than ≈ 0.4 radians, the error introduced is greater than 10%, and the other contributions to the sum rule begin to play an increasingly large role, further compounding this error. The asymmetry of the rotated Lorentzian is related to the Fano parameter q by $q^{-1} \propto \tan(\theta/2)$.

All the phonon lines have been fitted to Eq. 1 with a non-linear least-squares method. In addition to the parameters of the modified-Lorentzian oscillator, a linear background was used in the fits. We find that within the accuracy of our experiments, the four low-frequency lines are symmetric and only the 570 cm^{-1} line, and the new feature associated with it at 610 cm^{-1}, have clearly asymmetric shapes which become more pronounced at low temperatures.

It should be noted that if the Kramers-Kronig analysis is done on data that deviates from the true reflectance, for example by using room-temperature data for the high-frequency extrapolation for a low-temperature data set, there is a tendency for sharp lines to acquire an artificial asymmetry. As the experimental data become more accurate, the lines become more symmetric. The lines that have the highest reflectance are most susceptible to this error, which in our case is the 155 cm^{-1} line, which we find accurately symmetric, thus confirming the position of our 100% line. We find that an error of greater than 2% in the unity reflectance line would show an ob-

servable asymmetry.

The phonon parameters obtained by the least-squares fitting procedure applied to the rotated-Lorentzian profile with of all the measured spectra are assembled in Table I. We estimate the error in the parameters to be $\approx 1\%$ for the center frequencies, $\approx 5\%$ for the line widths, and $\approx 5\%$ for the effective plasma frequencies. Where there is a finite rotation angle θ, the error could be larger.

B. Assignment of phonons.

Group theory predicts seven B_{1u} infrared-active modes polarized in the c-direction for the fully-oxygenated orthorhombic (Ortho I) $YBa_2Cu_3O_7$ shown in Fig. 4.[40,41] There is crystallographic evidence that the oxygen-reduced material, with a plateau in the T_c vs x graph (in the $T_c \approx 60$ K region), has a doubled unit cell normal to the chain direction, resulting from an alternation of fully-occupied O(1) sites on chains with empty sites. This structure (Ortho II) is expected to have 13 infrared-active modes, but many of the new modes result from extremely small splittings of modes involving atoms far away from the chains. These small splittings may be partially responsible for the systematic broadening of most of the phonon lines at reduced dopings. We expect the largest changes for modes that involve atoms on and near the chains.

The assignment of the infrared-active spectral lines to normal modes is most reliable when the results from inelastic-neutron scattering are combined with a realistic lattice-dynamic model.[42] Such a procedure has been carried out recently for fully-oxygenated $YBa_2Cu_3O_7$,[§] and we make extensive use of the eigenvectors of these models in our discussion of c-axis the phonon spectra. A list of calculated contributions the various modes to the polarizability has been published by Timusk *et al.*[35] It is clear from the shell models that infrared modes, unlike Raman modes, which can often be assigned to the motion of a particular ion, usually involve the motion of all the ions in the unit cell. The shell-model eigenvectors suggest that there are some exceptions. For example the 570 cm^{-1} mode is almost a pure mode of the apical O(4) oxygen (a description of the different copper and oxygen environments is shown in Fig. 4). Similarly, the 279 cm^{-1} mode is an O(1) chain-oxygen vibration, polarized in the c-direction and the 315 cm^{-1} mode an O(2) and O(3) plane-bending vibration. The low-frequency modes involve many more atoms, and while the 194 cm^{-1} mode has been identified as the yttrium mode, it also involves substantial motion of the O(2) planar-oxygen atoms. The 155 cm^{-1} mode, often called the barium mode, according to the shell model gets more spectral weight from the

---

[§]W. Reichardt (private communication).

TABLE I. The parameters used to fit Lorentzian line shapes to the peaks in the optical conductivity of YBa$_2$Cu$_3$O$_{6+x}$, for $x = 0.95, 0.85, 0.7$, and 0.5 at 10 K. The two high-frequency copper-oxygen vibrations have been fitted using non-zero rotations.[a] (All parameters are in cm^{-1}).

$x = 0.95$				$x = 0.85$				$x = 0.7$				$x = 0.5$		
$\omega_{TO,i}$	γ_i	ω_{pi}		$\omega_{TO,i}$	γ_i	ω_{pi}		$\omega_{TO,i}$	γ_i	ω_{pi}		$\omega_{TO,i}$	γ_i	ω_{pi}
												93	11	116
				147	8.4	248		136	15	167		113	5.0	80
155	2.0	398	{				{	147	9.8	322	{	125	5.2	117
				153	3.8	351		153	4.2	267		145	9.0	363
												161	5.9	120
194	2.2	128	→	192	2.8	133	→	189	4.2	133	→	184	5.9	110
279	19	357	→	281	19	329	→	280	22	323	→	272	33	299
312	5.2	487	→	312	7.0	417	→	309	18	333	→	301	28	184
570	14	483	{	566	23	321	{	564	30	188	{	551	30	127
				619	23	205		630	24	250		637	24	251

[a]The two high-frequency apical-oxygen modes have been fit using a Lorentzian with a phase. The angles (in radians) used are: for $x = 0.95$, $\theta = -0.40, 0.0$, for $x = 0.85$, $\theta = -0.50, -0.15$, for $x = 0.7$, $\theta = -0.62, -0.45$, for $x = 0.5$, $\theta = -0.75, -0.80$, for the low and high-frequency components, respectively.
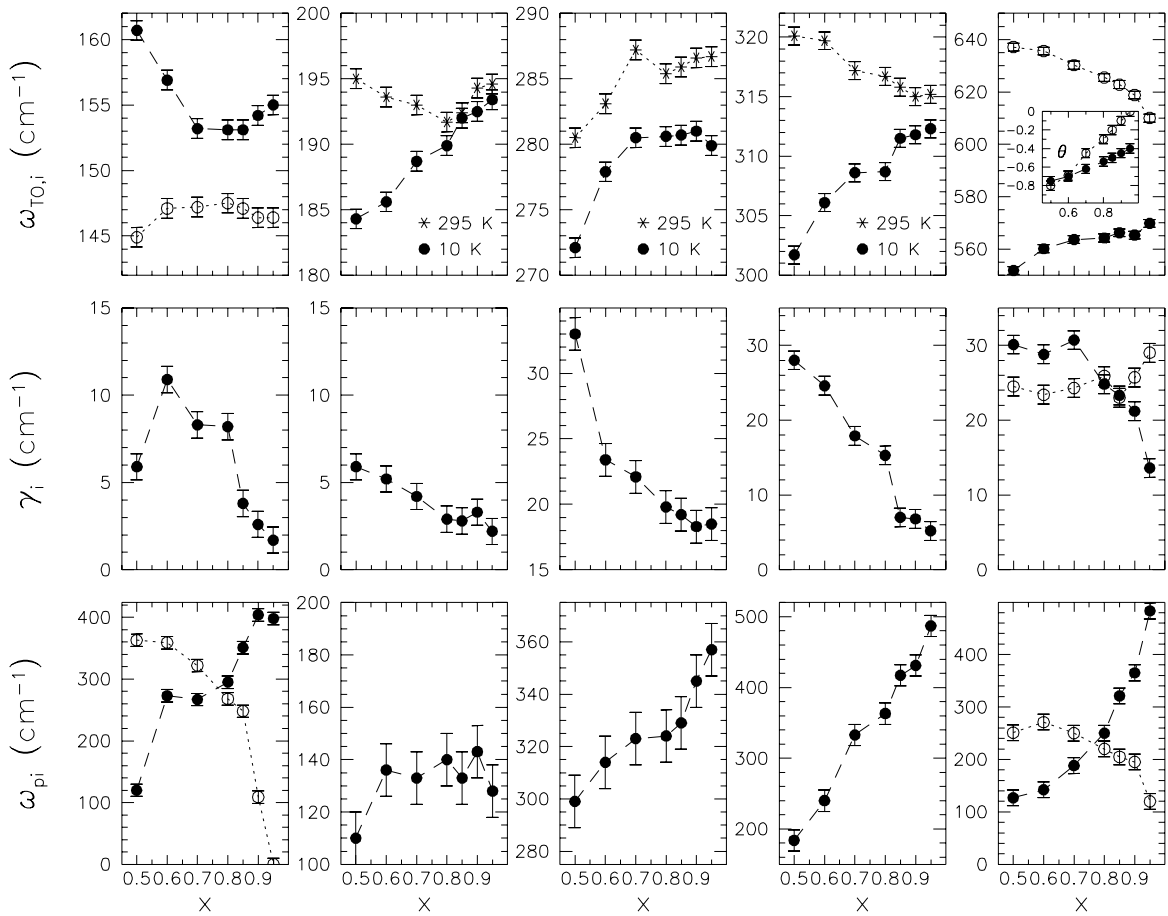

FIG. 5. The variation of the central frequency ($\omega_{TO,i}$), width (γ_i) and the effective plasma frequency (ω_{pi}) as a function of doping ($x = 0.5 \rightarrow 0.95$) of the five strong phonons observed in the highly-doped materials, at 10 K ($\bullet$). The room-temperature frequencies have been included for the three central panels ($*$). Also included in the panels are two phonons that appear only at lower oxygen dopings ($\circ$): in the first panel, at new mode appears at ≈ 148 cm^{-1} and gains oscillator strength as the mode observed in the highly-doped materials at ≈ 155 cm^{-1} becomes weaker. The second phonon appears at ≈ 610 cm^{-1} and, similarly to the 148 cm^{-1} phonons, gains oscillator strength with decreasing doping. Inset: rotation angles for the ≈ 570 cm^{-1} mode ($\bullet$), and the ≈ 610 cm^{-1} mode ($\circ$).
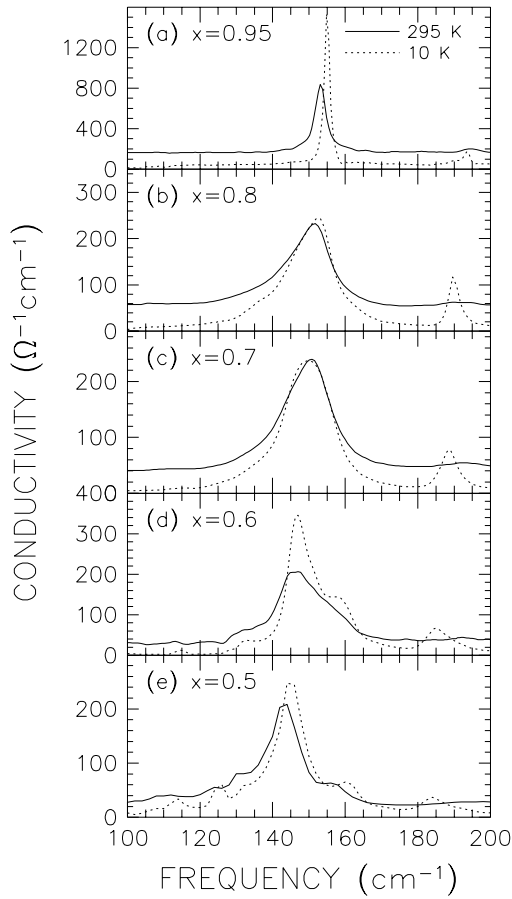
FIG. 6. The evolution of the shape of the 155 cm^{-1} line, at 295 K and 10 K, for five oxygen dopings ($x = 0.5 \rightarrow 0.95$). As the oxygen doping is reduced, the line broadens, first developing shoulders, and then finally splitting into several clearly resolved components.

TABLE II. The fitted phonon parameters for the c-axis B_{1u} modes in YBa$_2$Cu$_3$O$_{6.95}$ at 295 K determined from optical and inelastic neutron scattering measurements. The effective-plasma frequency based on the shell model with formal charges in column 5 [Y=+3.0, Ba=+2.0, Cu1=Cu2=2, O(1)=O(2)=O(3)=O(4)=-2] and fitted charges in column 6, [Y=+2.8, Ba=+2.5, Cu1=Cu2=2, O(1)=-1.8, O(2)=-1.8, O(3)=-.17, O(4)=-2.6]. (All units are in cm^{-1}.)

Optical[a]			Neutron[b]		
ω_{TOi}	γ_i	ω_{pi}	ω_i	ω_{pi}^{c}	ω_{pi}^{d}
—	—	—	111	100	115
153	3.6	389	149	283	330
—	—	—	186	22	14
195	3.7	95	198	79	94
287	18.3	316	291	455	400
315	15.6	498	322	493	457
568[e]	18.4	408	556	256	365

[a]Fitted to optical conductivity, this work.
[b]W. Reichardt *et al.*, private communication.
[c]Effective charges, formal valence charges
[d]Effective charges, fitted to optical data
[e]The high-frequency apical-oxygen mode has been fitted using an asymmetric line shape described by a Lorentzian with a rotation angle of $\theta = -0.27$ rad.

O(4) oxygen motion than from the barium, and also involves the motions of the Cu(1) and O(1) chain copper and oxygen atoms. This prediction is in agreement with our observation that this modes splits in oxygen-reduced materials.

In the highly-doped YBa$_2$Cu$_3$O$_{6.95}$ material five strong phonons are observed at 155, 194, 279, 312 and 570 cm^{-1} at 10 K. These frequencies are in excellent agreement with previous measurements on ceramics.[25,43] Table II compares these frequencies with those of the neutron-based shell model. As expected, since the $\boldsymbol{k} = \boldsymbol{0}$ frequencies have been fitted to the model, the agreement is satisfactory. What is surprising is the excellent agreement between the measured line strengths, and those predicted by the shell-model eigenvectors. In calculating the line strengths we have used two separate approaches: the simplest is to use the formal charges of the ions in all cases. The only case where this seems to be inappropriate is for the 570 cm^{-1} mode where the observed line strength is larger, and a larger effective charge on the O(4) would give better agreement between the model and the infrared

observations. This line is also anomalous in that it develops a strong asymmetry in the oxygen-reduced materials, a sign of strong electron-phonon interaction which may enhance the polarizability of the mode by dynamic charge transfer from the O(4) to the planes.

The second approach is to use a least-squares fit to the effective charges to the observed infrared oscillator strengths. The results are shown in column six of Table II. The fitted results, as expected, agree better with the optical data. However, it is interesting to note that in order to get this better fit, the main change was the removal of charge from the O(4) ion, and the addition of that charge on the planar oxygen ions.

The two missing lines are predicted by the shell model to be very weak. Of these there is some evidence for the lower one predicted to be at 111 cm^{-1} in some of our spectra, but they are near the limit of the accuracy of the experiments.

Two modes not predicted by the shell model are seen: the broad band at ≈ 400 cm^{-1}, and weak peak at ≈ 610 cm^{-1}. In what follows we will argue that the 610 cm^{-1} line is associated with the two-fold coordinated copper neighbor of the O(4) oxygen. Such sites are found in oxygen-reduced material where the 610 cm^{-1} line is much stronger, and its presence in our $x = 0.95$ sample is an indication that this sample contains a small concentration of broken chain fragments with two-fold coordinated copper.

Overall, at room temperature at least, there is good agreement with the shell model and the observed phonon spectrum and there is no need to invoke special electronic enhancements to explain the intensities of the phonon

lines, nor is there any evidence of strong screening by the electronic background.

C. Doping dependence of the phonon parameters

As the doping level is reduced, a number of changes in the phonon parameters take place; these are summarized for the five fundamental phonons observed in the highly-doped material, as well as the two strong splittings associated with the 155 cm^{-1} and 570 cm^{-1} modes at 10 K observed at lower dopings, in Fig. 5. To a first approximation one expects the phonon frequencies to soften with the expansion of the c-axis lattice parameter. One generally expects the frequency go approximately as the third power of the lattice parameter.[44] Since the c-axis lattice parameter increases by 0.5% between $x = 0.93$ to $x = 0.50$, one would expect an overall softening of the order of 1.5% as the result of the lattice expansion

In very rough agreement with this simple picture, many modes soften, but by a larger amount of 3.5% in this doping range. There are also several notable exceptions. First there is a tendency, at room temperature, for several modes to harden as the lattice expands on removal of oxygen, for example the 312 cm^{-1} mode. The 155 cm^{-1} mode as well as the high-frequency O(4) mode behave in a similar fashion: they split into two components, the higher frequency component hardens, the lower frequency one softens. As we will show below for the 570 cm^{-1} mode, and its high-frequency partner the 610 cm^{-1} mode the higher frequency component corresponds to the O(4) at the two-fold coordinated copper sites whereas the lower frequency corresponds to the O(4) at the four-fold coordinated copper sites. While the shell model eigenvectors suggest that the 155 cm^{-1} mode also involves a large amount of O(4) motion, many other atoms in the unit cell participate in the motion, and the net result is a behavior that is opposite to that for the 570 cm^{-1} mode: it is the high frequency, hard component that loses oscillator strength.

The mode at $\approx$ 155 cm^{-1} in the highly-doped material has split into a doublet in the $x = 0.85$ material, and consists of at least three lines in the $x = 0.7$ material; the phonon lines are significantly broader than the narrow line in the $x = 0.95$ material. Fig. 6 shows the evolution of the shape of this line with doping. The multi-component nature of the line and the gradual shift, with reduced doping to lower frequency components is reminiscent of the 500 cm^{-1} Raman line which has been shown to have many components, associated with chain disorder in underdoped samples.[45] The splitting of the $\approx$ 155 cm^{-1} mode is also associated with the loss of O(1) chain oxygens. Unlike the 570 cm^{-1} mode, where the O(4)-Cu(1) chain copper bond is stretched, the 155 cm^{-1} mode involves the O(4)-Cu(2) bond which is also expected to change its length as the Cu(1) changes from four to two-fold coordination.

As the doping decreases to $x \approx 0.7$, the 155 cm^{-1} O(4) mode softens and decreases in strength, while the mode at 148 cm^{-1} hardens slightly, and gains strength. Below $x \approx 0.7$, it is clear that the fundamental nature of this mode has changed; the 155 cm^{-1} feature hardens dramatically, and loses almost all of its oscillator strength; in contrast, the 148 cm^{-1} mode softens, and its oscillator strength approaches the value of the 155 cm^{-1} mode in the highly-doped material.

The 312 cm^{-1} plane-oxygen mode displays drastically different behavior at room temperature and at 10 K. At room temperature, the mode hardens from 315 cm^{-1} to 320 cm^{-1} and its oscillator strength remains unchanged as the doping is reduced. However, at 10 K, this mode softens dramatically with decreasing doping — furthermore, at $x \approx 0.5$ this mode, at low temperature, has lost most of its considerable oscillator strength. The loss of oscillator strength at low temperature in the underdoped materials results from the transfer of their spectral weight to the 400 cm^{-1} mode, which will be discussed in more detail below.

In the fully-oxygenated material the 610 cm^{-1} mode can just be seen as a weak side band of the 570 cm^{-1} mode, but as the doping is reduced the 610 cm^{-1} grows substantially in spectral weight. The mode hardens substantially to 645 cm^{-1} in the $x = 0.5$ material, while the 570 cm^{-1} mode that it is associated with is steadily losing oscillator strength with decreasing doping. This effect has been attributed by Burns *et al.* to the shortening of the O(4)-Cu(1) bond by 6% in the same concentration range.[46] In rough agreement with this model the 610 cm^{-1} line changes its frequency by 6% as well in the same concentration range. In Burns' picture the 570 cm^{-1} line arising from the O(4) at the four-fold coordinated copper, *softens* by 3%, a value typical of the overall c-axis expansion, suggesting a *lengthening* of that bond. If the interpretation of Burns is correct we would expect a modulation of the O(4) position in the a-direction by approximately 0.03 Å in the Ortho II structure where there is an alternation between two and four-fold coordinated coppers. There have been reports of a double peak in the Cu(1)–O(4) bond length distribution measured by XAFS by as much as 0.1 Å by several authors.[47–49]

The widths of the phonons increase steadily with decreasing doping, with the exception of the 155 cm^{-1} mode, which shows some signs of narrowing at low dopings. The steadily increasing widths may be a reflection of the O(1)-site disorder at low dopings. However, if there is some long-range ordering of the O(1) sites at low dopings, as is expected in the Ortho II phase, then there should be some narrowing observed in the lines. While there is some evidence of this in the 155 cm^{-1} mode, the 279 cm^{-1} mode shows no signs of narrowing at low-oxygen dopings.

The oscillator strengths are a convenient guide by which to follow the effects of the removal of oxygen from the O(1) sites. In particular, this is true for the 279 cm^{-1} mode, which is almost exclusively an O(1)-oxygen vibra-
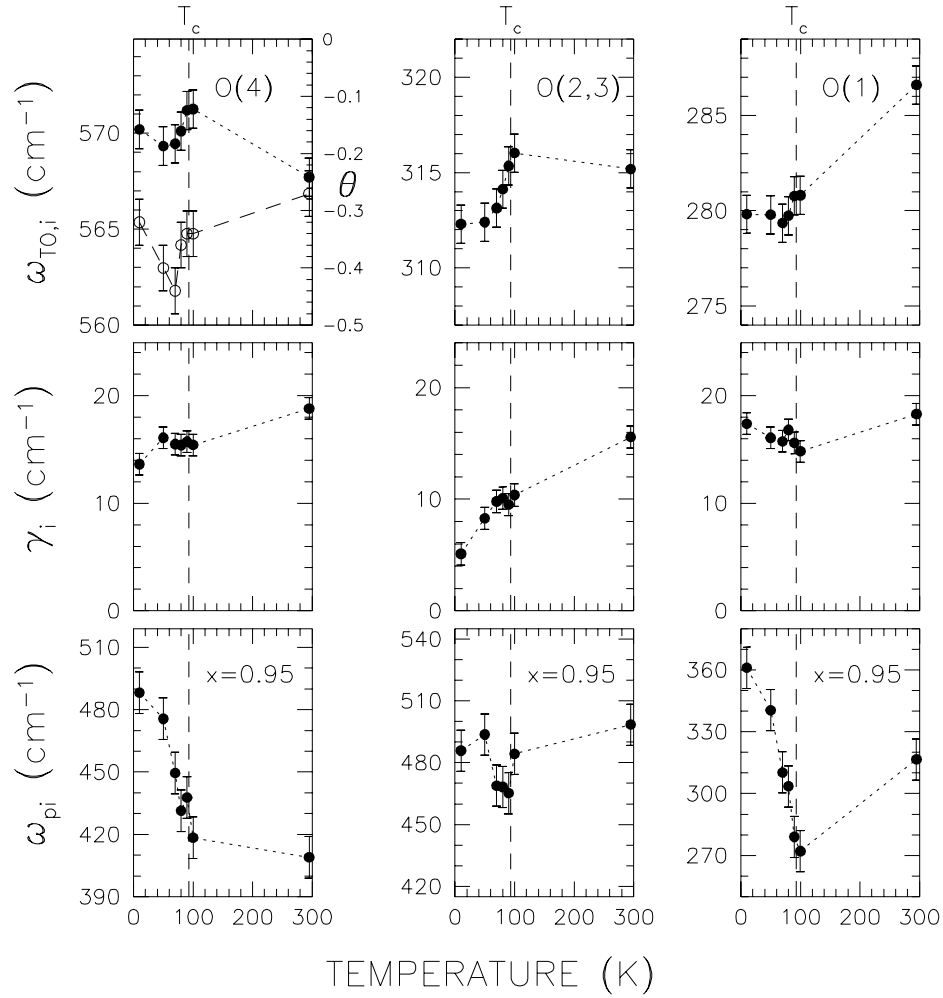
FIG. 7. The temperature dependence of the frequency ($\omega_{TO,i}$), line width (γ_i) and effective plasma frequency (ω_{pi}) for the three oxygen-related c-axis modes of YBa$_2$Cu$_3$O$_{6.95}$ (●). The ≈ 279 cm^{-1} mode fails to show any discontinuity at T_c, while the 312 cm^{-1} and 570 cm^{-1} modes both soften below T_c; the 570 cm^{-1} feature also appears to gain oscillator strength below T_c. The rotation angle used to fit the asymmetric line shape is shown in the O(4) panel (○), and shows a slightly increasing asymmetry with decreasing temperature.

tion. In the $x = 0.5$ material, we expect that the O(1) sites should be half empty. At 295 K, the effective-plasma frequency of this mode decreases from ≈ 310 cm^{-1} to ≈ 200 cm^{-1} in the $x = 0.5$ material; taking the naïve view that the ratio of the oscillator strengths ($\propto \omega_p^2$) of 0.44 should be a reflection of the half-empty occupancy of the O(1) sites, we find good agreement.

The asymmetric line shapes of the 570 cm^{-1} and 610 cm^{-1} modes require that they be fitted using a rotated Lorentzian. While this line shape generally satisfies oscillator sum rules for small rotations, it has been pointed out that for large rotations ($\theta > 0.4$ rad) this is no longer true. The values for ω_p may generally have increasingly large errors associated with them for large rotations. The results show a decreasing oscillator strength for the 570 cm^{-1} with decreasing doping, and the 610 cm^{-1} mode show a steadily increasing oscillator strength with de-

creasing doping with the two oscillator strengths becoming equal at $x = 0.7$. Below $x \approx 0.6$, the 610 cm^{-1} line appears to be decreasing in intensity. This latter result is consistent with the small value for ω_p observed in the tetragonal YBa$_2$Cu$_3$O$_6$ material.

D. Temperature dependence of the phonon parameters.

The temperature dependence of the phonon parameters for the three high-frequency modes in YBa$_2$Cu$_3$O$_{6.95}$ is shown in Fig. 7, the results are in general agreement with previous work.[12–15] The temperature dependence for the four high-frequency modes in YBa$_2$Cu$_3$O$_{6.7}$ is shown in Fig. 8.
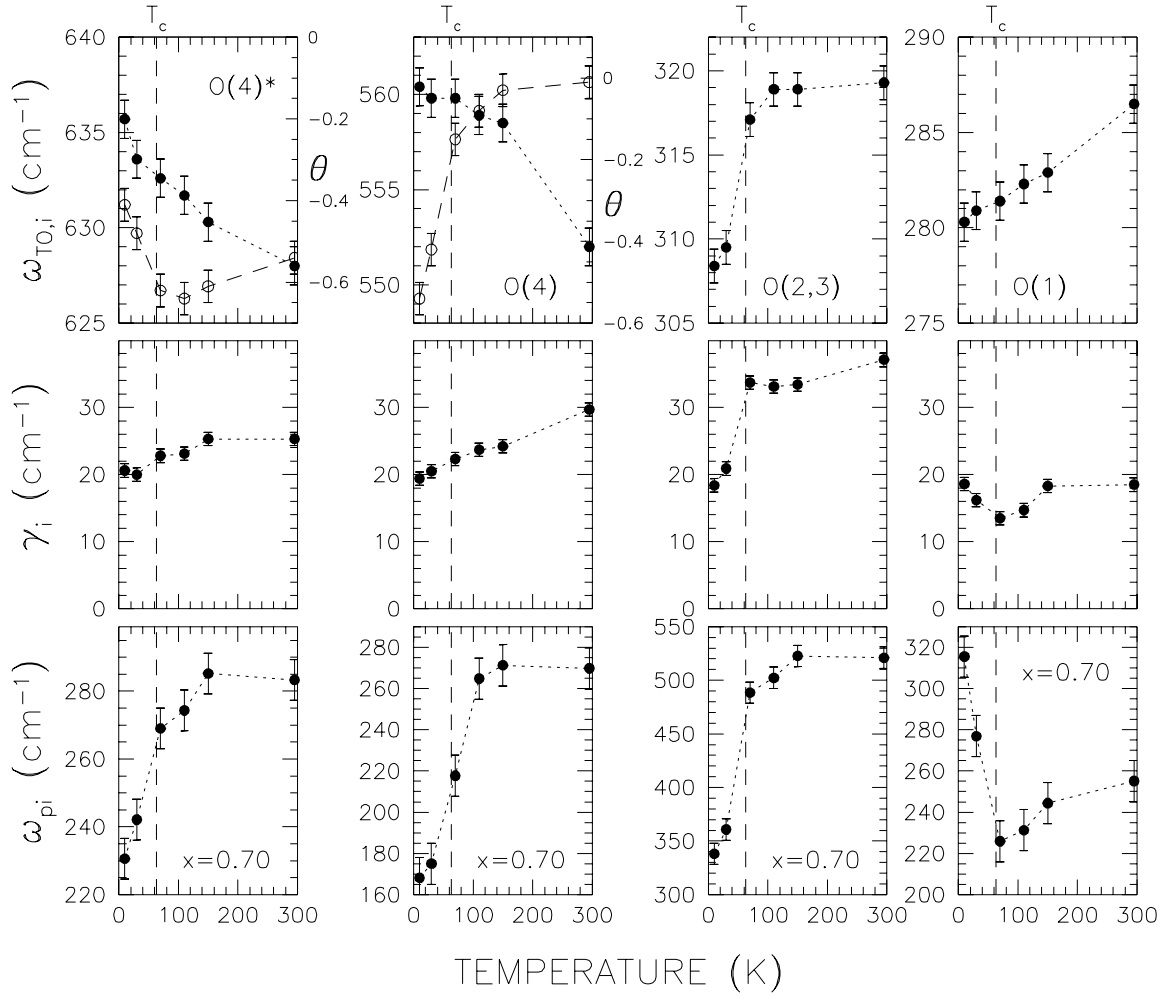
In the highly-doped material, as the temperature is

FIG. 8. The temperature dependence of the frequency ($\omega_{TO,i}$), line width (γ_i), and effective plasma frequency (ω_{pi}) for the three oxygen-related c-axis modes of $YBa_2Cu_3O_{6.70}$, and a new fourth feature associated with the change in coordination of the Cu(1) atom, discussed in the text (●). The feature at ≈ 285 cm^{-1} softens with decreasing temperature, while the two modes at ≈ 557 cm^{-1} and ≈ 630 cm^{-1} harden smoothly — the feature at 318 cm^{-1} softens well above T_c. The three high-frequency modes begin to loose oscillator strength at ≈ 150 K, while the low-frequency mode gains in strength primarily below T_c. The rotation angles (o) used to fit the two high-frequency modes are shown in the O(4)* and O(4) panels: the ≈ 570 cm^{-1} mode becomes increasing asymmetric at low temperature, while the mode at ≈ 610 cm^{-1} becomes more symmetric.

lowered, the phonon frequencies generally increase due to anharmonic effects, but there are exceptions, most notably the 279 cm^{-1} chain-oxygen mode, which softens by ≈ 6 cm^{-1} between 295 K and 10 K. The two low-frequency modes display little temperature dependence. The mode at ≈ 155 cm^{-1} hardens slightly from 153 cm^{-1} at room temperature to 155 cm^{-1} at 10 K. The feature at ≈ 194 cm^{-1} softens to 193 cm^{-1} at 10 K; this feature shows a slight anomaly at T_c.

The three remaining modes at 279, 312 and 570 cm^{-1} are all associated with oxygen vibrations, and show a more dramatic behavior. The 312 cm^{-1} mode and the 570 cm^{-1} mode both harden with decreasing temperature, but show a discontinuity and soften below T_c. The peak at ≈ 279 cm^{-1}, originally associated with the oxy-

gen atoms in the CuO_2 planes, has been reassigned as an O(1) chain-oxygen vibration;[50] this mode softens continuously from room temperature to below T_c, and shows only a weak anomaly at T_c. However, like the 570 cm^{-1} mode, the 279 cm^{-1} mode shows some signs of hardening below ≈ 40 K. The line widths of the 279 cm^{-1} mode shows only a weak temperature dependence, while the line widths of the 312 cm^{-1} and 570 cm^{-1} modes both narrow with decreasing temperature — interestingly, none show any sign of anomalous behavior at T_c.

There is substantial variation in the oscillator strengths with temperature. The 279 cm^{-1} feature weakens considerably with decreasing temperature, but then becomes much stronger below T_c, while the 312 cm^{-1} remains relatively constant. The O(4) mode at 570 cm^{-1}

shows a rapid increase in oscillator strength at T_c, and initially becomes more asymmetric below T_c, suggesting the possibility of electron-phonon coupling (all the other modes have been fit using simple Lorentzian oscillators).

The sharpness of the phonons in the highly-doped phase, especially at the low frequency modes at 155 cm^{-1} and 279 cm^{-1}, where anharmonic contribution to the width is small, is a sign of good crystal quality. In previous single crystal work with polished samples, these features were broad and weak, suggesting either poor oxygen homogeneity, or that polishing the sample has induced surface damage or altered the oxygen content of the material in the surface layers, particularly in the chains. Furthermore, an examination of the reflectance of polished c-axis crystals[30,31] shows that they bear a strong similarity to the reflectance of freshly-annealed ceramics.

The 194 cm^{-1} mode, according to the shell model, has its eigenvectors confined to plane region of the unit cell, and therefore does not split when alternate chains become deoxygenated, as expected.

The vibrations at 279 cm^{-1} and 312 cm^{-1} in the highly-doped material harden and soften slightly with decreasing oxygen content, respectively, while also broadening considerably.

The temperature dependence of the phonon parameters in the oxygen-reduced system is dramatically different from the fully-doped case. As Fig. 8 shows for YBa$_2$Cu$_3$O$_{6.70}$ there is now an additional mode at ≈ 610 cm^{-1}. The two apical-oxygen modes at 557 cm^{-1} and 630 cm^{-1} harden continuously with decreasing temperature, and there is no sign of a phonon anomaly at the superconducting transition temperature. As noted by Litvinchuck[14] the plane feature at ≈ 318 cm^{-1} displays very interesting behavior in that it begins to soften rapidly at ≈ 100 K, well above the T_c of 63 K. The chain feature at ≈ 285 cm^{-1} at room temperature softens to ≈ 279 cm^{-1} at low temperature — none of these features shows any discontinuity at T_c.

The behavior of the line widths is similar to that of the oscillator strengths. The strengths of the two high-frequency modes both begin to decrease at ≈ 140 K, well above T_c, as does the strength of the ≈ 312 cm^{-1} mode. This is in sharp contrast to the ≈ 279 cm^{-1} mode, which loses strength with decreasing temperature until T_c, at which point it begins to increase very rapidly — this is the only feature which shows any sensitivity to T_c.

The rapid loss of oscillator strength, particularly in the 312 cm^{-1} mode in the $x = 0.7$ material is even more noticeable in the $x \lesssim 0.6$ materials: in the $x = 0.5$ material, this mode appears to have completely collapsed at 10 K. The mode at ≈ 410 cm^{-1} (or combination of modes), which is very weak in the $x = 0.95$ material, is gradually becoming stronger as the oxygen content is decreased, so that in the oxygen-reduced $x = 0.6$ material, it is one of the dominant features. Furthermore, as the other oxygen related vibrations are losing oscillator strength, this feature is becoming correspondingly stronger, as Fig. 9 illustrates. Interestingly, optical sum-
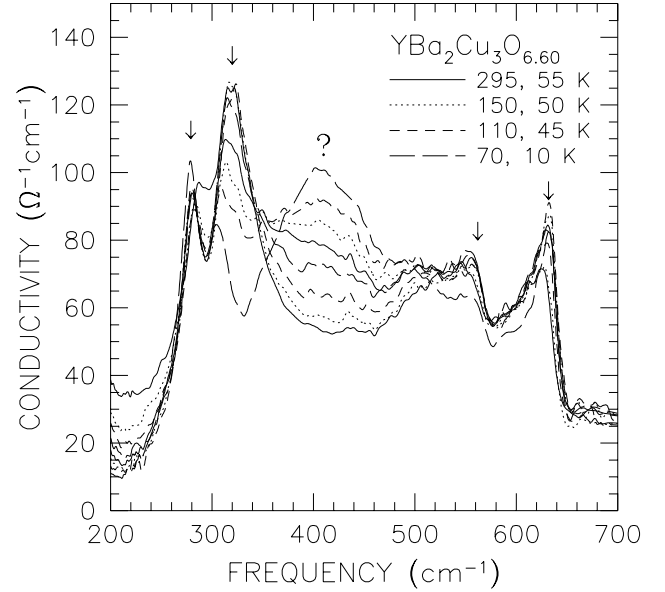

FIG. 9. The optical conductivity (σ_1) of YBa$_2$Cu$_3$O$_{6.60}$ along the c-axis as a function of temperature, from 200 cm^{-1} to 700 cm^{-1}, for four temperatures each above and below T_c (≈ 58 K). Note the dramatic loss in the strength of the feature at ≈ 318 cm^{-1}, and the corresponding increase in the feature (or group of features) centered at ≈ 400 cm^{-1} — there is no anomalous behavior near T_c.

rule calculations show no net increase or decrease in the spectral weight in the $250 - 700$ cm^{-1} region, suggesting that the ≈ 400 cm^{-1} feature(s) is growing as a result of the transfer of oscillator strength for the other modes, but in particular from the planar copper-oxygen vibrations. The ≈ 400 cm^{-1} feature is identifiable well above T_c, and appears to grow smoothly, and without any sudden discontinuity at T_c. Furthermore, the 312 cm^{-1} mode loses a great deal of oscillator strength, and begins to do so well above T_c. This suggests that while there is a major reorganization of the vibrational energy in the CuO$_2$ planes (in the oxygen-reduced materials) as the temperature is lowered; this is a separate mechanism which may affect superconductivity in these materials, but does not appear to be affected by the superconducting transition. Interestingly, similar behavior is observed in the high-frequency copper-oxygen vibrations in cupric oxide (CuO) near the Néel transition.[51]

IV. DISCUSSION

A. The assignment of the 610 cm^{-1} phonon.

The most striking change at room temperature with doping, is the growth of the 610 cm^{-1} mode at the ex-

10

pense of the 570 cm^{-1} mode. This 610 cm^{-1} feature has been observed in other work and has been the subject of some controversy, since there is lack of agreement in the Raman community on the presence of the corresponding Raman mode at 600 cm^{-1}.[52] In the tetrahedral YBa$_2$Cu$_3$O$_6$ material, which lacks the O(1) oxygen chains, there is an infrared active A_{2u} mode that is observed at $645-650$ cm^{-1} which, like the 573 cm^{-1} mode in the orthorhombic phase, has been identified with the O(4) oxygen.[53] In removing the chain oxygens, the fourfold coordinated Cu(1) "squares" become two-fold coordinated "sticks".[52] The change in coordination number is accompanied by a decrease in the Cu(1)-O(4) distance, and a resulting hardening of the mode causing it to move from 570 cm^{-1} to 610 cm^{-1}.[52] The feature at ≈ 610 cm^{-1} therefore appears to be an A_{2u} mode native to the tetrahedral phase involving the O(4)-Cu(1)-O(4) sticks.

In accord with this picture we find that the oscillator strength of the two modes, at 570 cm^{-1} and 610 cm^{-1}, are nearly identical in the $x = 0.70$ material. One expects the ideal Ortho II structure to occur at $x = 0.50$ where there are an equal number of two and four-fold coordinated coppers with every other chain complete and every other chain empty. Also, the temperature dependence of the various mode parameters seen in Fig. 8, is nearly identical for the two modes confirming that they are located on nearly identical structural units.

Some recent Raman work does show intensity variation with doping that parallels our work with weakening of the 500 cm^{-1} line as the 600 cm^{-1} line grows. The two lines reach lines of equal strength at 500 cm^{-1} and 600 cm^{-1} in the oxygen reduced, $x = 0.75$ material.** Surprisingly, this is observed for the $\boldsymbol{E} \parallel \boldsymbol{b}$ polarization.

Neutron measurements, too, find a mode in oxygen-reduced material $x = 0.25$ at $\boldsymbol{q} = \boldsymbol{0}$ at the frequency that is consistent with Burns' model of a high frequency mode for two-fold coordinated Cu(1).[54] It should also be noted that the neutron density of states determined by incoherent scattering shows a high frequency band of modes in the $x = 0$ phase centered at 650 cm^{-1}, whereas the fully-doped material has its highest branch at ≈ 575 cm^{-1},[55] in accord with the notion of a set of high-frequency modes associated with the oxygen-reduced material.

B. The 400 cm^{-1} mode.

Another trend with decreasing doping is the appearance and growth of a broad band at ≈ 400 cm^{-1} at low temperature. The band also shifts to lower frequencies as the doping is reduced. As shown in Fig. 3 and in Fig. 9, this unusual feature increases in strength in the normal state as the temperature is lowered, but does not

---

**M.N. Iliev, private communication

show anomalous behavior at T_c. At very low dopings, $(x \lesssim 0.6)$ where this band is quite strong, it appears to gain oscillator strength at the expense of the 312, 570, and 610 cm^{-1} phonons. At room temperature where the phonons are sharp and well defined, the total spectral weight of the in the $250 - 700$ cm^{-1} range, is equal to the total spectral weight, including the 400 cm^{-1} mode, at low temperature. This conservation of spectral weight is consistent with the idea that the broad peak at ≈ 400 cm^{-1} is indeed a phonon.

The broad, weak mode at ≈ 408 cm^{-1} has been observed in ceramic spectra of samples that appear to have been oxygen reduced,[12] but this mode does not correspond to any of the calculated B_{1u} normal modes.[40,41] A similar mode is seen in YBa$_2$Cu$_4$O$_8$[56] as well as in Pb$_2$Sr$_2$RCu$_3$O$_8$.[57] The common element in the three compounds is the third copper layer with two-fold coordinated oxygen bonds. In all three systems the mode appears at low temperature, growing in strength at the expense of both in-plane mode at 312 cm^{-1} as well as the two apical-oxygen modes. This behavior suggests that an unusual transition is taking place that involves several atoms in the unit cell. The transition may be related to the zone-boundary mode reported on by Reichardt *et al.*;[58] located at approximately 400 cm^{-1}, it was found to be anomalously broad and involved the "breathing" motions of the ions around the planar copper. This mode is not normally infrared active, but could become so as a result of some symmetry-breaking process. The mode involves the c-axis motion of the O(4), but not the in-plane motion of the planar oxygens. Its invocation would explain only half of our observations, namely the loss of O(4) spectral weight to the new mode through an electron-phonon process of the type discussed in connection with organic molecules by Rice.[59] In such a process a symmetry-breaking transformation allows totally-symmetric vibrations (here the zone-boundary breathing mode) to become optically active. A necessary ingredient of the process is the presence of low-lying charge-transfer bands. The excess spectral weight and the asymmetric shape of the O(4) bands suggests that charge is being pumped at the O(4) frequency between chains and planes. This process is already active at high temperature above the formation temperature of the pseudo-gap. It would then not be unreasonable to anticipate that when the symmetry-breaking transition sets in at 150 K in the oxygen-reduced materials, that some of this phonon-driven charge is transferred from the O(4) and plane modes, to the newly activated breathing mode. The difficulty with this argument is that it is does not apply to the other two compounds where this mode is observed.[56,57]

Possibly related to this unusual phonon, polarized in the c-direction, is the phenomenon in the ab plane conductivity reported on by Reedyk and Timusk where, in YBa$_2$Cu$_3$O$_{6.95}$ the c-axis longitudinal modes interacted strongly with the ab plane conductivity.[60,61] The strongest of these was a broad phonon with the longitu-

dinal frequency of 440 cm^{-1}.

The structural transition giving rise to the phonon at ≈ 400 cm^{-1} band appears to be related to the pseudogap seen at ≈ 280 cm^{-1} in underdoped materials. It is strong in underdoped materials where the pseudogap is also well developed. In Zn-doped YBa$_2$Cu$_4$O$_8$, both the pseudogap and the 400 cm^{-1} mode disappear at a 1.7% doping level.[††] However, there are some differences. Whereas the pseudogap appears gradually, in case of the $x = 0.6$ material at a temperature well above 300 K, the 400 cm^{-1} band forms quite suddenly at ≈ 150 K, as shown by the sudden loss of O(4) spectral weight below this temperature.

In summary, at this stage we have only the vaguest understanding of the nature of the phonons giving rise to the band at 400 cm^{-1}, it is a feature that appears at low temperature in oxygen-reduced materials only, and gets its oscillator strength from plane-buckling and the O(4) modes. Its frequency coincides with the anomalous broad mode seen in neutron scattering, and a broad minimum in the ab-plane conductivity. Zn doping of YBa$_2$Cu$_4$O$_8$ seems to interfere with the formation of this mode. It should be noted that it is not the result of a simple structural transition, since the *frequencies* of the modes involved change little – there is no soft mode behavior. It appears that the transition is electronic in nature, the main result being the shift of effective charges of the phonons, not their frequencies.

V. CONCLUSIONS

The phonons in the oxygen-reduced systems provide a richly detailed structure. At high dopings, there are five strong B_{1u} modes. At low dopings ($x \lesssim 0.7$), many of the lines split into a number of different components. In particular, the high-frequency apical-oxygen mode splits into two components; the low-frequency component is associated with the four-fold coordinated copper atom, and the high-frequency component with the two-fold coordinated copper. What is most unusual is the development of a broad feature, centered at ≈ 400 cm^{-1}. This feature, attributed to a (unknown) phonon, becomes more pronounced as oxygen is removed from the system; it grows in strength as the temperature is lowered, appearing to draw oscillator strength from the vibrations at ≈ 320, 570 and 610 cm^{-1} with decreasing temperature. This behavior develops well above T_c, and other phonon anomalies are seen in the $x = 0.7$ material at ≈ 150 K.

Since these massive shifts of spectral weight to the 400 cm^{-1} mode are not seen in other high-temperature superconductors, such as La$_{2-x}$Sr$_x$CuO$_4$ and Bi$_2$Sr$_2$CaCu$_2$O$_{8+z}$,[62,63] they may be related to some special structural property of materials with a third copper layer in the charge reservoir area of the unit cell, and not a fundamental property of the cuprates.

[††]D.N. Basov, T. Timusk and B. Dabrowski (unpublished)

---

[*] Accepted for publication in a special issue of the Canadian Journal of Physics in honour of B.N. Brockhouse.

[†] Present Address: Department of Physics, Simon Fraser University, Burnaby, B.C., Canada V5A 1S6, Email: homes@sfu.ca

[‡] Corresponding author, Tel: (416) 978-5199, FAX: (416) 978-2537, Email: timusk@mcmaster.ca

[1] M. Gurvitch and A.T. Fiory, Phys. Rev. Lett. **59**, 1337 (1987).

[2] S.M. Martin, A.T. Fiory, R.M. Fleming, L.F. Schneemeyer, and J.V. Waszcak, Phys. Rev. B **41**, 846 (1990).

[3] D.B. Romero, C.D. Porter, D.B. Tanner, L. Forro, D. Mandrus, L. Mihaly, G.L. Carr, and G.P. Williams, Phys. Rev. Lett. **68**, 1590 (1992).

[4] D.A. Bonn, R. Liang, P. Dosanjh, and W.N. Hardy, Phys. Rev. Lett. **68**, 2390 (1992).

[5] R.C. Yu, M.B. Solomon, J.P. Lu, and W.C. Lee, Phys. Rev. Lett. **69**, 1431 (1992).

[6] B. Batlogg *et al.*, Phys. Rev. Lett. **58**, 2333 (1987).

[7] L.C. Bourne *et al.*, Phys. Rev. Lett. **58**, 2337 (1987).

[8] J.P. Franck, J. Jung, G.J. Salomons, W.A. Miner, M.A.-K. Mohammed, J. Chrzanowski, S. Gygax, J.C. Irwin, D.F. Mitchell, and G.I. Sproule, Physica C **172**, 90 (1990).

[9] M.K. Crawford, M.N. Kunchar, W.E. Farneth, E.M. McCarron III, and S.J. Poon, Phys. Rev. B **41**, 282 (1990).

[10] For a recent review of infrared-active vibrations in high-temperature superconductors, see A.P. Litvinchuk, C. Thompsen and M. Cardona, *in* Physical Properties of High-Temperature Superconductors IV. *edited by* D.M. Ginsberg, World Scientific, Singapore, 1992, pp. 375-470.

[11] For a recent review of phonon properties measured by neutron scattering see L. Pintschovius and W. Reichardt, *ibid.* pp. 295-374.

[12] D.A. Bonn, J.E. Greedan, C.V. Stager, T. Timusk, M.G. Doss, S.L. Herr, K. Kamarás, D.B. Tanner, Phys. Rev. Lett. **58**, 2249 (1987).

[13] A. Wittlin, R. Liu, M. Cardona, L. Genzel, M. Bauer, W. König, and E. Garcia-Alvarado, Solid State Commun. **64**, 477 (1987).

[14] A.P. Litvinchuk, C. Thomsen, and M. Cardona, Solid State Commun. **83**, 343 (1992).

[15] R.M. Macfarlane, H. Rosen, and H. Seki, Solid State Commun. **63**, 831 (1987).

[16] B. Friedl, C. Thomsen, and M. Cardona, Phys. Rev. Lett. **76**, 1107 (1990).

[17] E. Altendorf, X.K. Chen, J.C. Irwin, R. Liang, and W.N. Hardy, Phys. Rev. B **47**, 8140 (1993).

[18] H.A. Mook, M. Mostoller, J.A. Harvey, N.W. Hill, B.C. Chakoumakos, and B.C. Stales, Phys. Rev. Lett. **69**, 2712 (1990).

[19] N. Pyka, W. Reichardt, L. Pintschoviius, G. Engel, J. Rossat-Mignod, and J.Y. Henry, Phys. Rev. Lett. **70**, 1457 (1993).

[20] T. Timusk, C.D. Porter and D.B. Tanner, Phys. Rev. Lett. **66**, 663 (1991).

[21] M. Reedyk and T. Timusk, Phys. Rev. Lett. **69**, 2705 (1992).

[22] C.C. Homes, T. Timusk, D.A. Bonn, R. Liang and W.N. Hardy, (unpublished)

[23] J. Schützmann, S. Tajima, S. Miyamoto, and S. Tanaka, Phys. Rev. Lett. **73**, 174 (1994).

[24] Optical properties in the c-direction are reviewed by S.L. Cooper and K.E. Gray, *in* Physical Properties of High-Temperature Superconductors IV, *edited by* D.M. Ginsberg, World Scientific, Singapore, 1992, pp. 61-188.

[25] D.A. Bonn, A.H. O'Reilly, J.E. Greedan, C.V. Stager, T. Timusk, K. Kamarás, and D.B. Tanner, Phys. Rev. B **37**, 1574 (1988).

[26] L. Genzel, A. Wittlin, M. Bauer, M. Cardona, E. Schönherr, and A. Simon, Phys. Rev. B **40**, 2170 (1989).

[27] R. Feile, Physica C **159**, 1 (1989).

[28] I. Bozovic, D. Kirillov, A. Kapitulnik, K. Char, M.R. Hahn, M.R. Beasley, T.H. Geballe, Y.H. Kim, and A.J. Heeger, Phys. Rev. Lett. **59**, 2219 (1987).

[29] R.T. Collins, Z. Schlesinger, F. Holtzberg, and C. Feild, Phys. Rev. Lett. **63**, 422 (1989).

[30] B. Koch, M. Dürrler, Th. Wolf, G. Roth, G. Zachmann, Solid State Commun. **71**, 495 (1990).

[31] B. Koch, M. Dürrler, H.P. Geserich, Th. Wolf, G. Roth, and G. Zachmann, *in* Electronic Properties of High-T_c Superconductors and Related Compounds. *Edited by* H. Kuzmany, M, Mehrig, J. Fink, Springer Series in Solid State Sciences, Vol. 99, Springer-Verlag, Berlin-Heidelberg, 1990, p. 290.

[32] S.L. Cooper, P. Nyhus, D. Reznik, M.V. Klein, W.C. Lee, D.M. Ginsgerg, B.W. Veal, A.P. Paulikas, and B. Dabrowski, Phys. Rev. Lett. **70**, 1533 (1993); S.L. Cooper, D. Reznik, A. Kotz, M.A. Karlow, R. Liu, M.V. Klein, W.C. Lee, J. Giapintzakis, D.M. Ginsberg, B.W. Veal, and A.P. Paulikas, Phys. Rev. B **47**, 8233 (1993).

[33] C.C. Homes, T. Timusk, R. Liang, D.A. Bonn, and W.N. Hardy, Phys. Rev. Lett. **71**, 1645 (1993).

[34] T. Timusk, C.C. Homes, N. Cao, and D.B. Tanner, Anisotropic Optical Conductivity of YBa$_2$Cu$_3$O$_{7-\delta}$, *in* Proceedings of the Bejing International Conference on High-Temperature Superconductivity (BHTSC '92), *Edited by* Z.Z. Gan, S.S. Xie, and Z.X. Zhao, World Scientific, Singapore, 1993, pp. 408–415.

[35] T. Timusk, C.C. Homes, and W. Reichardt, *in* Int. Workshop on the Anharmonic Properties of High-T$_c$ Cuprates, Bled, Slovenia. *Edited by* G. Ruani, World Scientific, Singapore, 1995).

[36] R. Liang, P. Dosanjh, D.A. Bonn, D.J. Baar, J.F. Carolan, and W.N. Hardy, Physica C **195**, 51 (1992).

[37] C.C. Homes, M.A. Reedyk, D.A. Crandles, and T. Timusk, Appl. Opt. **32**, 2976 (1993).

[38] V.M. Burlkov, K.V. Kraiskaya, A.G. Mitko, E.J. Firsov, Phys. Lett. A **142**, 514 (1989); V.M. Burlkov, N.Y. Boldyrev, I. Gaiduk, K.V. Kraiskaya, A.G. Mitko, Pis'ma Zh. Eksp. Teor. Fiz. **52**, 733 (1990); JETP Lett. **52**, 91 (1990).

[39] U. Fano, Phys. Rev. **124,** 1866 (1961).

[40] F.E. Bates and J.E. Eldridge, Solid State Commun. **64**, 1435 (1987).

[41] W. Kress, U. Schröder, J. Prade, A.D. Kulkarni, and F.W. de Wette, Phys. Rev. B **39**, 2906 (1988).

[42] R.A. Cowley, W. Cochran, B.N. Brockhouse, and A.D.B. Woods, Phys. Rev. **131,** 1030 (1963).

[43] M.K. Crawford, W.E. Farneth, E.M. McCarron III, and R.K. Bordia, Phys. Rev. B **38**, 11382 (1988).

[44] V.A. Maroni, T.O. Brun, M. Grimsditch, and C.-K. Loong, Phys. Rev. B **39**, 4127 (1989).

[45] V. Hadjiev, C. Thomsen, J. Kircher, and M. Cardona, Phys. Rev. B **47**, 9148 (1993).

[46] For a compilation of lattice parameters of high-temperature superconductors see R.M. Hazen, The crystal structure of high T_c superconductors, *in* Physical Properties of High-Temperature Superconductors II. *Edited by* D.M. Ginsberg, World Scientific, Singapore, 1990, p. 121–198.

[47] S.D. Conradson, I. Raistrick, and A.R. Bishop, Science **248**, 1934 (1990).

[48] J. Mustre de Leon, S.D. Conradson, I. Batisitić, and A.R. Bishop, Phys. Rev. Lett. **65**, 1675 (1990).

[49] E.A. Stern, M. Quian, Y. Yakoby, S.M. Heal, and H. Maeda, Physica C **209**, 331 (1993).

[50] C. Thomsen, A.P. Litvinchuk, E. Schönherr, and M. Cardona, Phys. Rev. B **45**, 8145 (1992).

[51] C.C. Homes, M. Ziaei, B.P. Clayman, J.C. Irwin, and J.P. Franck, Phys. Rev. B **51**, 3140 (1995).

[52] G. Burns, F.H. Dacol, C. Feild, and F. Holtzberg, Physica C **181**, 37 (1991).

[53] G. Burns, F.H. Dacol, P.P. Freitas, W. König, and T.S. Plaskett, Phy. Rev. Lett. **37**, 5171 (1988).

[54] N. Pyka (unpublished results, quoted in Ref. 11)

[55] B. Renker, F. Gompf, E. Gering, D. Ewert, H. Rietschek, and A. Dianoux, Z. Phys. B – Condensed Matter **73**, 309 (1988).

[56] D.N. Basov, T. Timusk, B. Dabrowski, and J.D. Jorgensen, Phys. Rev. B **50**, 3511 (1994).

[57] M. Reedyk, T. Timusk, J.S. Xue, and J.E. Greedan, Phys. Rev. B **49**, 15984 (1994).

[58] W. Reichardt, N. Pyka, L. Pintschovius, B. Hennion, and G. Collin, Int. Conf. on Superconductivity, Stanford, 1989, Physica C **162–164**, 464 (1989).

[59] M.J. Rice, V.M. Yartsev,and C.S. Jacobsen, Phys. Rev. B **21**, 3437 (1980).

[60] T. Timusk, C.D. Porter and D.B. Tanner,Phys. Rev. Lett. **66**, 663 (1991).

[61] M. Reedyk and T. Timusk, Phys. Rev. Lett. **69**, 2705 (1992).

[62] K. Tamasaku, T. Itoh, H. Takagi, and S. Uchida, Phys. Rev. Lett. **72**, 3088 (1994).

[63] S. Tajima, G.D. Gu, S. Miyamoto, A. Odagawa, and N. Koshizuka, Phys. Rev. B **48**, 16164 (1993).